INPP5D (SHIP1)

A Target Enabling Package (TEP)

Gene ID / UniProt ID / EC	3635 / Q92835 / 3.1.3.86
Target Nominator	AMP-AD
Authors	William Bradshaw[1], Richard Priestley[2], Juliane Obst[2], Hazel Hall-Roberts[2], Anna Cederbalk[2], Paul Brennan[2], Emma Mead[2], Elena Di Daniel[2], John Davis[2] Opher Gileadi[1]
Target PI	Opher Gileadi
Therapeutic Area(s)	Alzheimer's Disease
Disease Relevance	Non-coding SNP rs35349669 increases risk of Alzheimer's, the protein is part of the PIP signalling pathway, which has been linked to neuroinflammatory risk.
Date Approved by TEP Evaluation Group	November 27th 2020
Document version	1.0
Document version date	November 2020
Citation	William Bradshaw, Richard Priestley, Juliane Obst, Hazel Hall-Roberts, Anna Cederbalk, , Paul Brennan, … Opher Gileadi. (2020). SH2-containing-inositol-5-phosphatases (INPP5D); A Target Enabling Package [Data set]. Zenodo. http://doi.org/10.5281/zenodo.4429248
Affiliations	[1]SGC, University of Oxford [2]Oxford Drug Discovery Institute, University of Oxford

USEFUL LINKS

GeneCards HUMAN GENE DATABASE | Open Targets | 50 YEARS OMIM Human Genetics Knowledge for the World | ChEMBL | Agora

(Please note that the inclusion of links to external sites should not be taken as an endorsement of that site by the SGC in any way)

SUMMARY OF PROJECT

SH2-containing-inositol-5-phosphatases (SHIP1 and SHIP2, coded for by genes *INPP5D* and *INPPL1*, respectively) dephosphorylate phosphatidylinositol-3,4,5-trisphosphate ($PI(3,4,5)P_3$) to produce phosphatidylinositol-3,4-bisphosphate ($PI(3,4)P_2$). This is an important part of the PI3K/AKT/mTOR signalling pathway. The SHIPs have been linked to a range of conditions, including cancer(1-3) diabetes (4), hypertension (5), and graft versus host disease (6). A link has also been demonstrated by GWAS between a non-coding mutation in the *INPP5D* (SHIP1) gene and increased risk of late-onset Alzheimer's disease. The role of SHIP1 in Alzheimer's disease is believed to be mediated through inflammatory processes such as the regulation of microglia and cytokine release (7,8). The distinction between the effects of SHIP1 and SHIP2 on these processes is not fully understood. In this TEP we present an apo structure of the phosphatase and C2 domains of SHIP1 and a structure with a magnesium ion and a phosphate ion bound to the active site. We also present 91 fragment bound structures that may act as starting points for the modulation of SHIP1. We are also able to crystallise an equivalent construct of SHIP2 and purify a range of other inositol-5-phosphatases to serve as a selectivity panel for the development of specific compounds. An assay has also been developed.

SCIENTIFIC BACKGROUND

The human genome codes for ten inositol-5-phosphatases, all of which are believed to primarily convert $PI(3,4,5)P_3$ to $PI(3,4)P_2$. The active site is generally well conserved within the family, although there are differences in their levels of activity (9). The primary method by which the functions of the inositol-5-phosphatases are delineated seems to be through differing levels of expression in various tissues (10-12). Despite this, there is some evidence of overlapping roles (13).

rs35349669, a non-coding SNP in the SHIP1 gene has been shown to increase the risk of late-onset Alzheimer's disease (14). SHIP1 has been implicated in neuroinflammatory processes within the brain, specifically through regulation of microglia and cytokine release (7,8). It is through these processes that the link to Alzheimer's is believed to be mediated, although it has also been suggested that SHIP2 may be involved (13).

Clearly, an improved understanding of the how the two SHIPs carry out their functions and their respective roles in Alzheimer's disease and other conditions is required, alongside a broader understanding of the related roles of all ten inositol-5-phosphatases. To this end, a number of inhibitors and activators that can be used as probes have been developed in recent years, some of which are reported to have near-equal efficacy on the two SHIPs, while others are selective (13,15,16). The utility of many of these compounds is somewhat limited and better probes, particularly ones that have been structurally engineered to have high affinities and to be selective, would prove invaluable

RESULTS – THE TEP

Proteins purified

Various constructs have been cloned for 7 of the 10 human inositol-5-phosphatases. Of these, constructs coding for at least the phosphatase domain of INPP5D (SHIP1), INPPL1 (SHIP2), INPP5A, INPP5B, INPP5E, SKIP1 (INPP5K) and SYNJ1 can be expressed and purified. Other inositol phosphatases including PTEN, INPP4A, INPP4B and INPP1A have also been cloned, expressed and purified to serve as a selectivity panel for the development of novel and selective compounds. INPP5D and INPPL1 are 52% identical in the phosphatase-C2 domains, with near-identity in the catalytic site, and we expect particular challenges in developing selective inhibitors.

The two primary constructs code for the phosphatase and C2 domains of SHIP1 (INPP5DA-c232, E396-Q856) and SHIP2 (INPPL1A-c231, E420-R878) and can be purified to a high degree (**Fig 1**), with a yield of approximately 1 mg per litre expressed and 2 mg per litre expressed for SHIP1 and SHIP2, respectively.

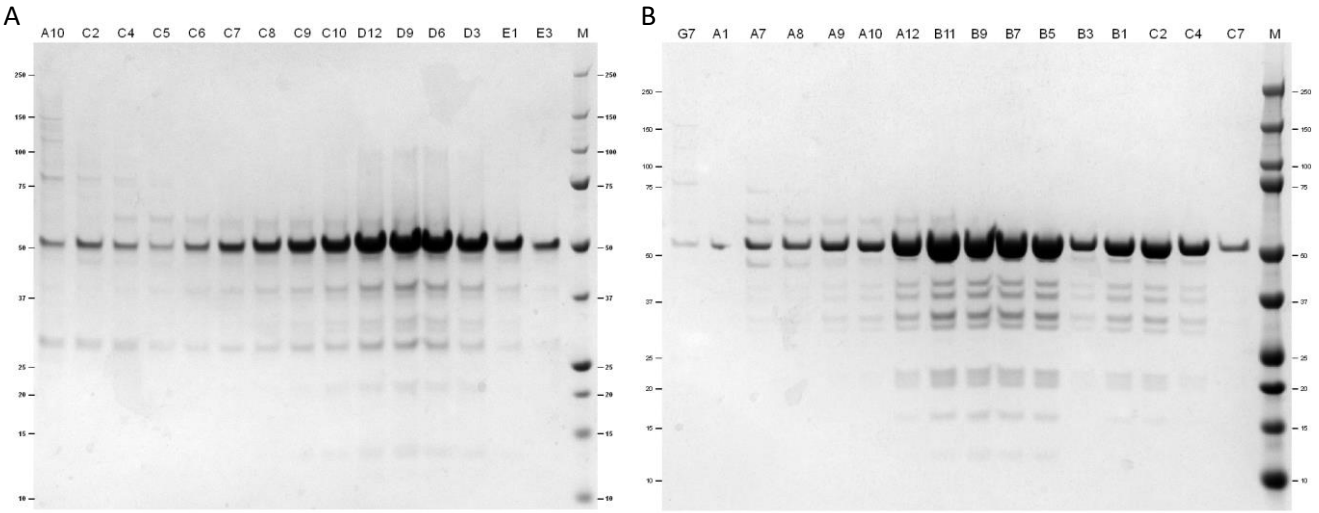

Figure 1. Gel filtration chromatograms **(A)** INPP5DA-c232, the phosphatase and C2 domains of SHIP1 **(B)** INPPL1a-c231, the phosphatase and C2 domains of SHIP2.

Structural Data

Crystallisation conditions have been established for INPP5DA-c232 and INPPL1A-c231. Crystals grown in these conditions routinely diffract to a high resolution. A SHIP1 apo structure at 1.48 Å (6IBD) and a structure with magnesium and phosphate bound to the active site at 1.09 Å (6XY7) have been deposited in the PDB (**Fig 2**). An X-ray fragment screen was performed on SHIP1 and 108 binding events were observed (**Fig 3**). These can be viewed in Fragalysis. While no fragments were observed to be bound to the active site, several were seen in a pocket near to the interface between the phosphatase and C2 domains, including two fragments covalently bound to C505. As the C2 domain is believed to modulate activity of the phosphatase domain (10,17), it is possible these fragments could be used as starting points for the development of compounds that may be able to disrupt the allosteric effect of the C2 domain.

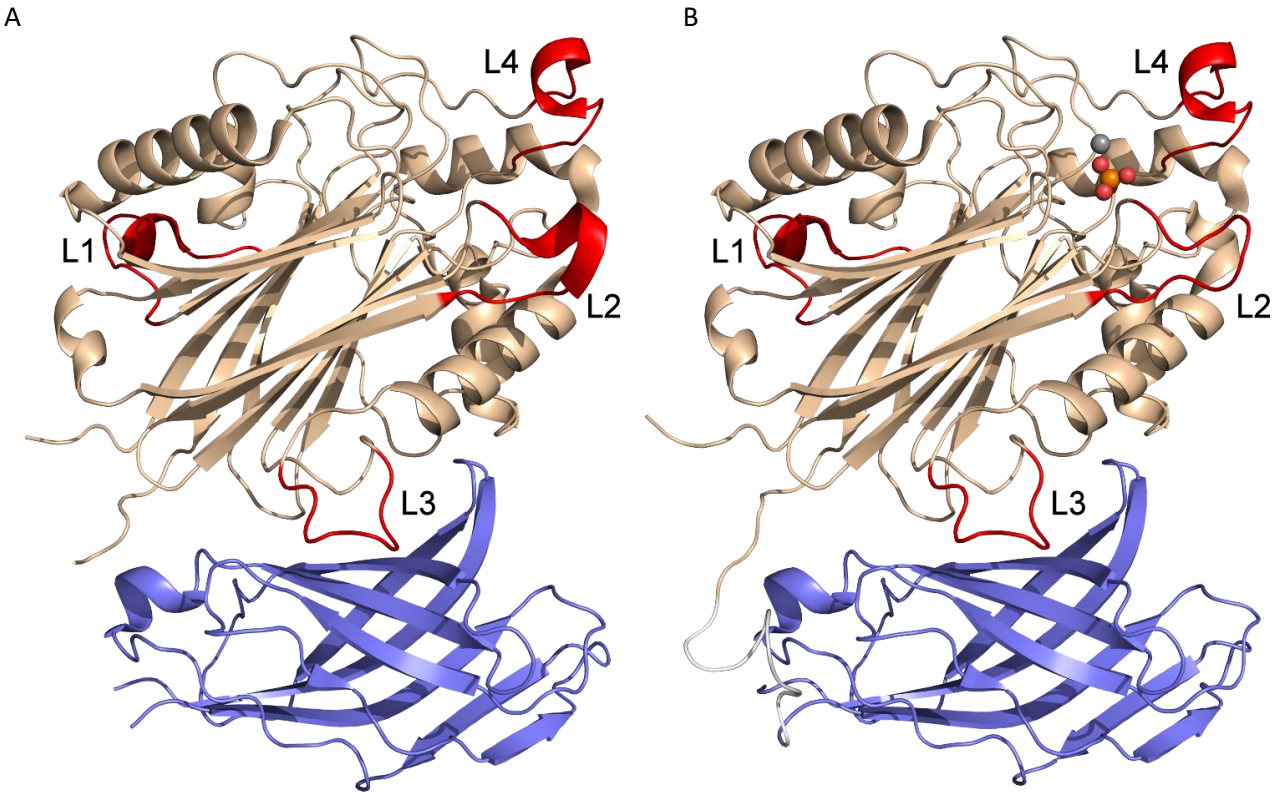

Figure 2. High resolution structures of the phosphatase and C2 domains SHIP1 **(A)** The 1.48 Å apo structure. The phosphatase domain is coloured in brown, the C2 domain in blue. Functionally important loops noted by Le Coq *et al*. (2017) are highlighted in red. **(B)** The magnesium and phosphate bound structure of SHIP1. Colouring follows that of A. The magnesium ion and phosphate ion are shown bound to the active site.

Assays

A biochemical assay has been established for INPP5DA to measure its catalytic activity against phosphatidylinositol (3,4,5)-trisphosphate - aka PI(3,4,5)P_3, through the detection of free orthophosphate product using the Malachite Green detection method. In brief, the assay works through the quantification of the green complex formed between Malachite Green, molybdate, and free orthophosphate as detected via absorbance at 620 nm. The assay is able to detect the production of free phosphate by the enzyme in a concentration-dependent manner, as well as detect the activity of the known INPP5DA inhibitor 3α-aminocholestane – aka 3AC (**Fig 3**).

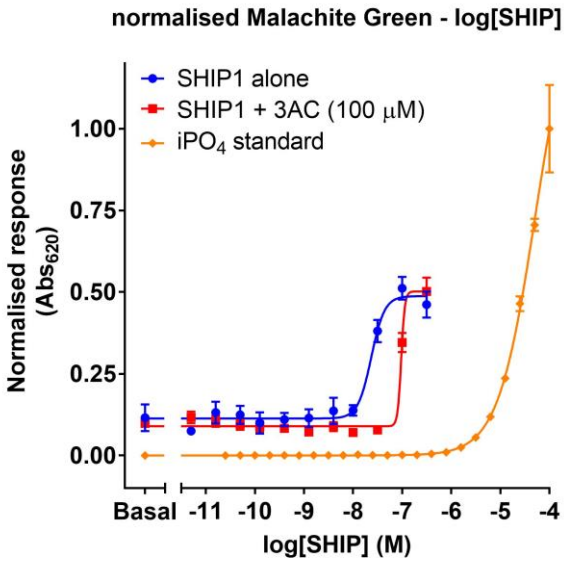

Figure 3. Representative figure for INPP5DA (SHIP1) Malachite Green catalytic activity assay. The substrate is present at 25 μM.

Chemical Matter

A crystal-based fragment screen yielded clusters of small molecules which were mostly bound at the protein surface and in crystallisation interfaces.

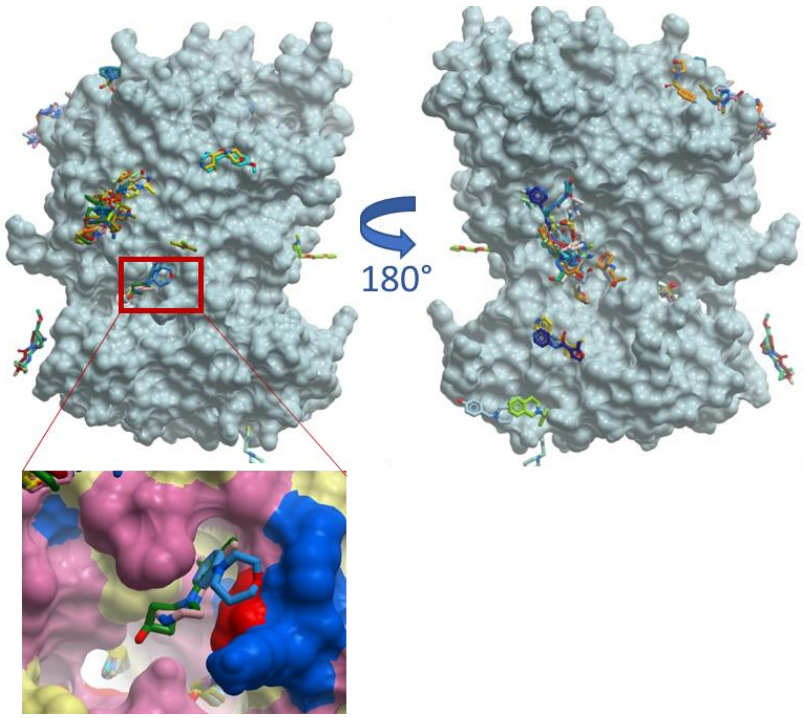

Figure 4. 108 binding events were observed for 92 compounds. The majority were crystallographic artefacts (in contacts between neighbouring proteins in the crystal), but a small number were located in site 3, near the interface between the phosphatase and the C2 domains (inset), including two fragments that were bound covalently to Cys 505. It may be possible to use these fragments as starting points for compounds that could allosterically affect the enzymatic activity.

IMPORTANT: Please note that the existence of small molecules within this TEP indicates only that chemical matter might bind to the protein in potentially functionally relevant locations. The small molecule ligands are intended to be used as the basis for future chemistry optimisation to increase potency and selectivity and yield a chemical probe or lead series. As such, the molecules within this TEP should not be used as tools for functional studies of the protein, unless otherwise stated, as they are not sufficiently potent or well-characterised to be used in cellular studies.

Future plans

Forty follow-up compounds have been designed based upon the fragments bound at the interface between the phosphatase and C2 domains. 72 Compounds suspected to be able to bind to the active site have also been identified by Atomwise using *in silico* methods. Both sets of compounds will be screened crystallographically against both SHIP1 and SHIP2 to identify those able to bind to either protein. Activity assays will be used to measure any modulatory effect the compounds have. Compounds will be further optimised using iterative crystallographic methods and activity assays, with a particular focus on compounds that are active against SHIP1 and not the other inositol phosphatases in the selectivity panel.

CONCLUSION

The structures of SHIP1 presented here allow comparison to that of SHIP2 and other inositol 5-phosphatases. Any differences between them should be considered as possible avenues to explore for the development of novel and selective compounds to moderate their activity. While the structures of SHIP1 and SHIP2 are very similar, there are some potentially important differences. The two proteins appear to differ more in the C2 domain than the phosphatase domain. The fragment bounds structures may serve as starting points for the development of novel compounds able to modulate the interaction between the phosphatase and C2 domains, thereby affecting the activity of the phosphatase domain. A biochemical assay (Malachite green) has been established and validated for screening, which will enable the identification of novel SHIP1 modulators, and can be used in hit-confirmation activities from the fragment screen.

TEP IMPACT

This work has lead a degree of collaboration with Purdue/Indiana TREAT-AD team, who are also working on SHIP1 and with the Potter lab, Department of Pharmacology, University of Oxford and Charles Brearley, UEA, who have developed a range of artificial SHIP2 substrates.

A manuscript of the work presented here is currently being written.

FUNDING INFORMATION

The work performed at the SGC has been funded by NIH grants 1RF1AG057443-01 and 1U54AG065187-01 and Wellcome grant [106169/ZZ14/Z].

ADDITIONAL INFORMATION

Structure Files

PDB ID	Structure Details
6IBD	Apo structure of the phosphatase and C2 domains
6XY7	Phosphatase and C2 domains with magnesium and phosphate bound

Fragments and PDB depositions

Note: only fragments in site 3 are seen as relevant for further development.

PDB ID	Ligand	Binding location	Binding pocket	Resolution (Å)

5RW2	x0019 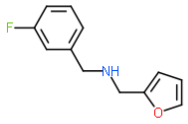	Site 01 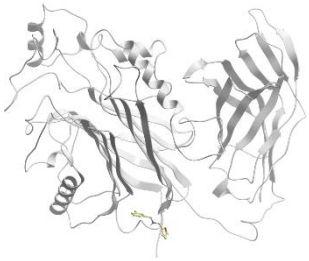	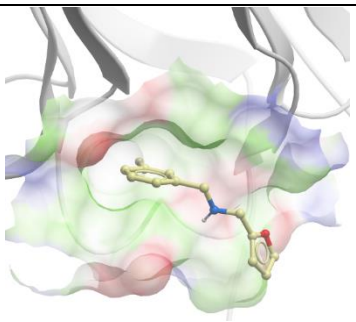	1.22
5RW4	x0021 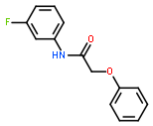	Site 01 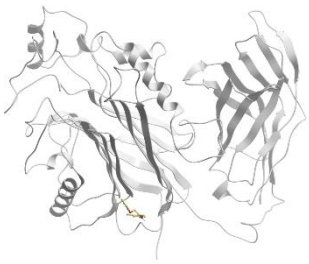	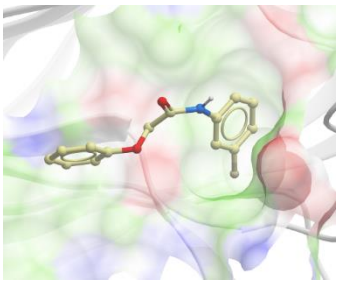	1.31
5RW6	x0030 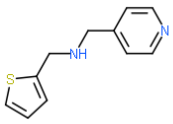	Site 01 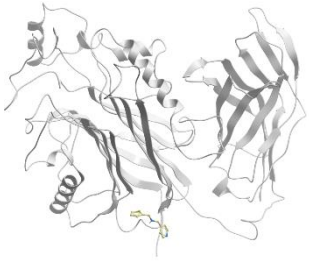	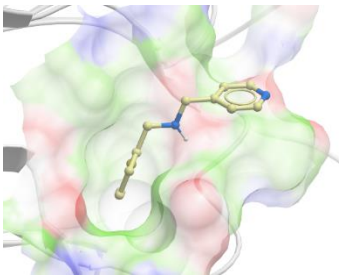	1.32
5RW7	x0039 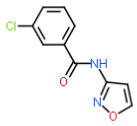	Site 01 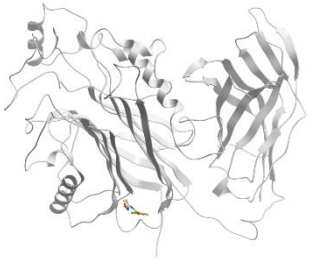	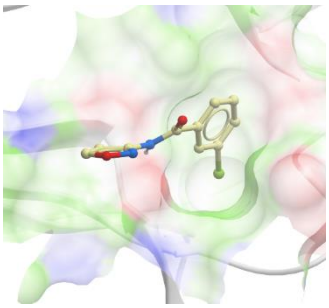	1.23
5RW8	x0040 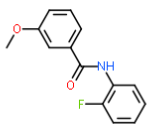	Site 01 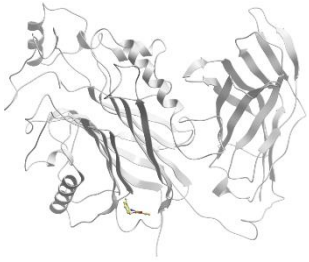	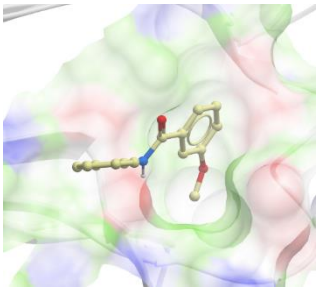	1.27
5RW9	x0054 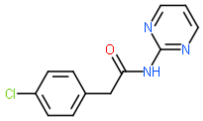	Site 01 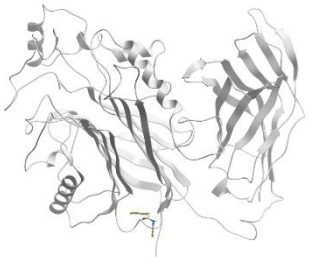	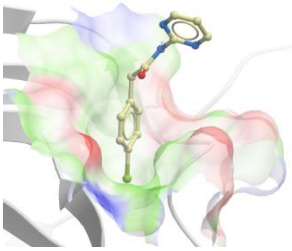	1.45

5RWG	x0084 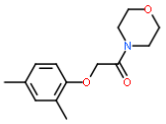	Site 01 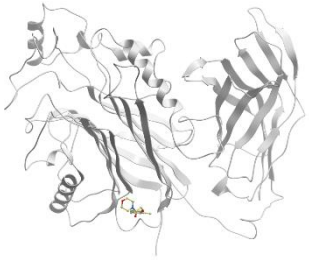	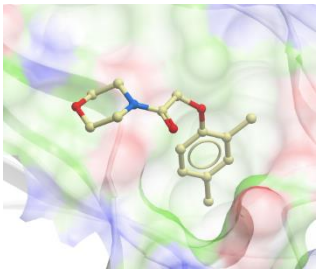	1.46
5RWJ	x0097 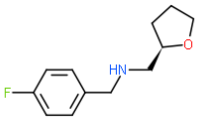	Site 01 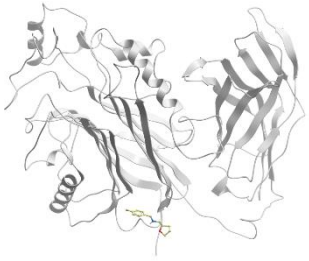	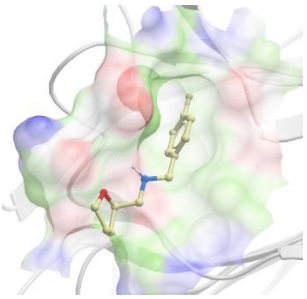	1.26
5RWK	x0100 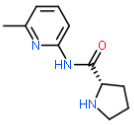	Site 01 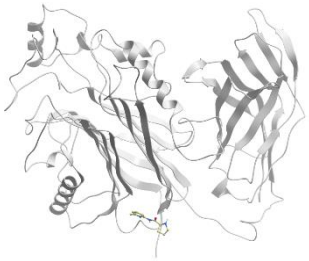	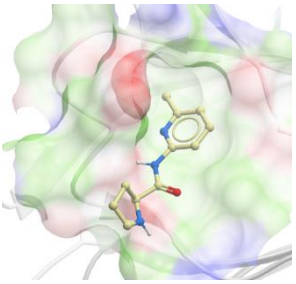	1.32
5RWP	x0118 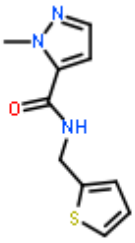	Site 01 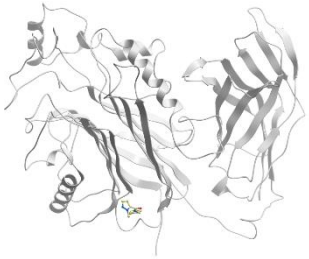	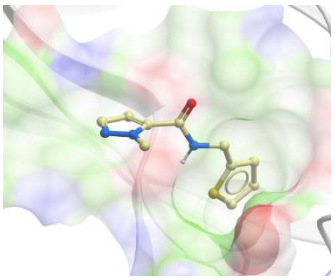	1.48
5RWR	x0121 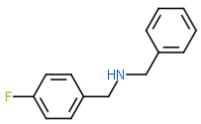	Site 01 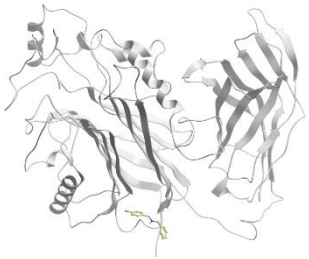	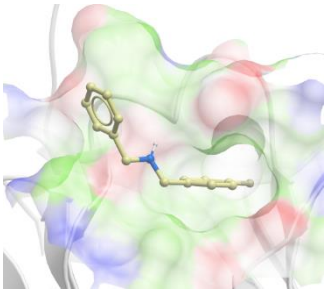	1.43

5RX2	x0169 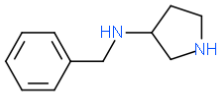	Site 01 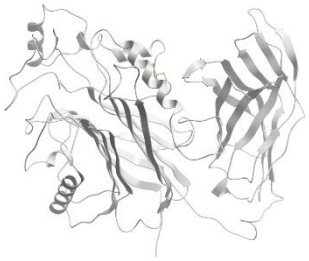	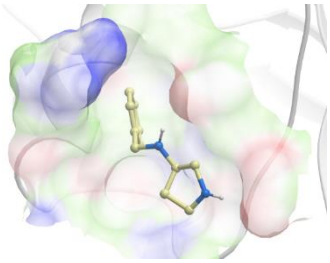	1.27
5RX6	x0183 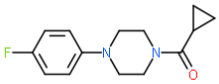	Site 01 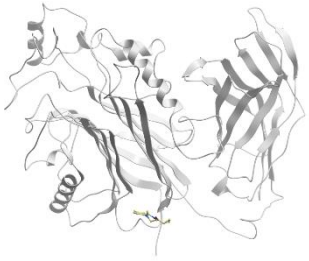	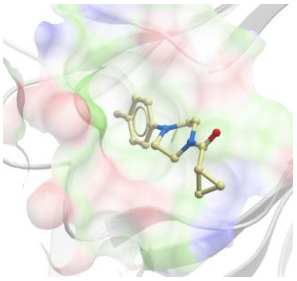	1.45
5RXD	x0243 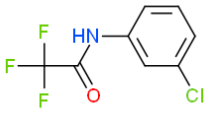	Site 01 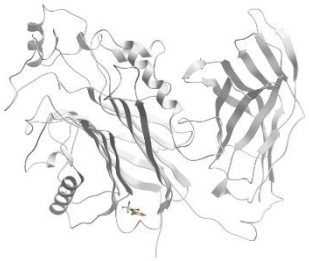	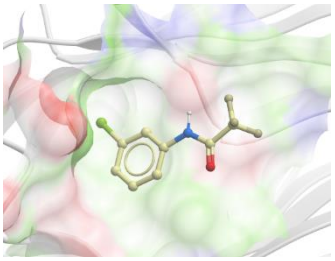	1.33
5RXE	x0251 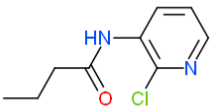	Site 01 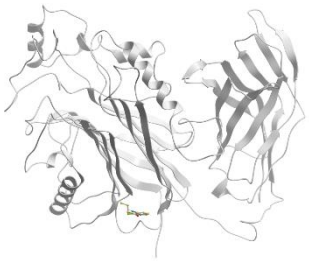	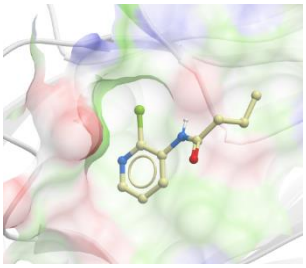	1.25
5RXF	x0300 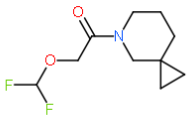	Site 01 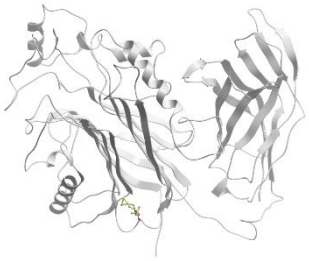	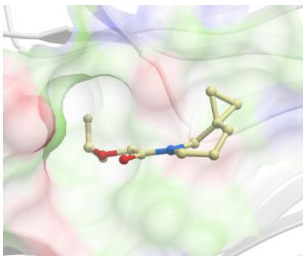	1.26
5RXO	x0342 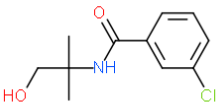	Site 01 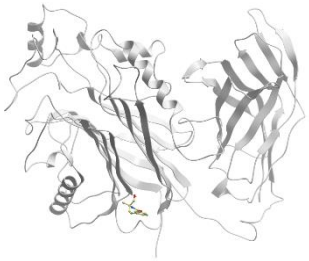	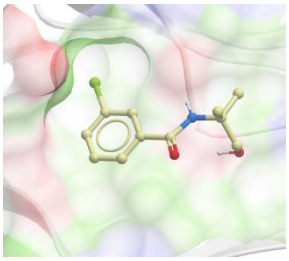	1.71

5RXP	x0345 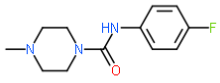	Site 01 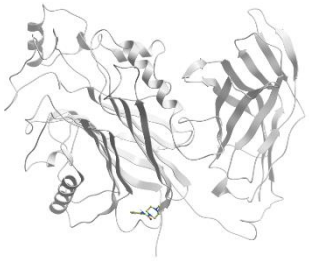	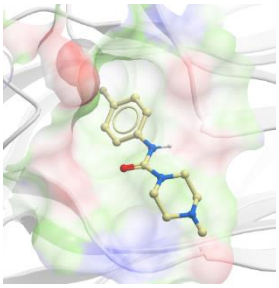	1.53
5RXQ	x0350 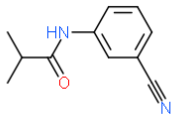	Site 01 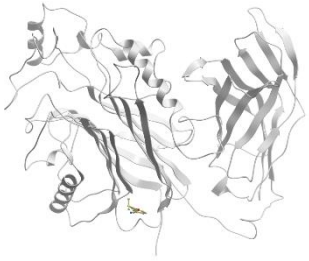	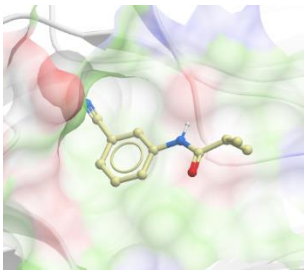	1.65
5RXT	x0361 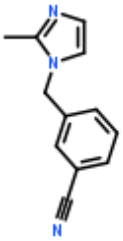	Site 01 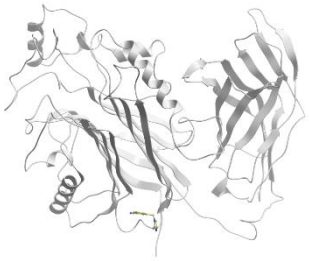	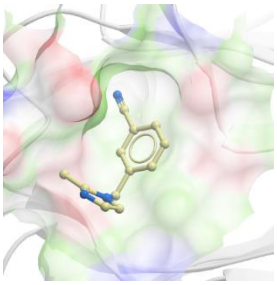	1.63
5RXW	x0382 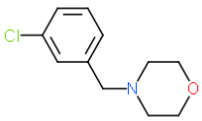	Site 01 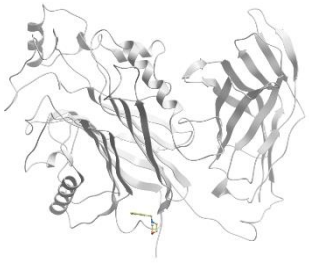	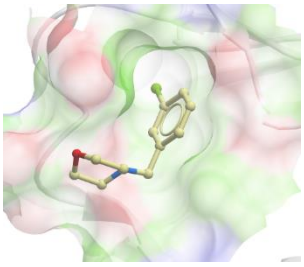	1.34
5RXZ	x0417 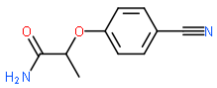	Site 01 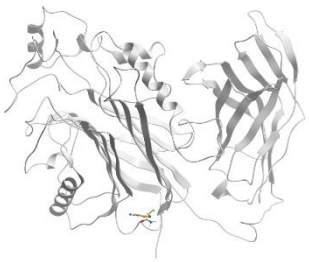	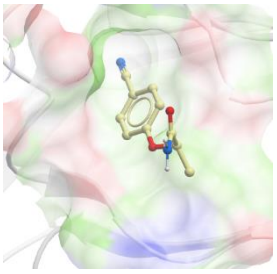	1.56

5RY0	x0423 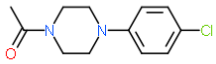	Site 01 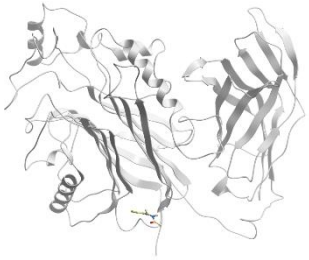	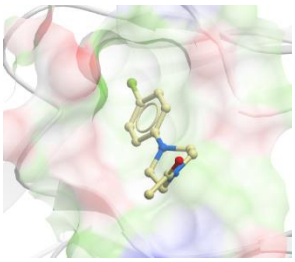	1.98
5RY2	x0449 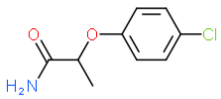	Site 01 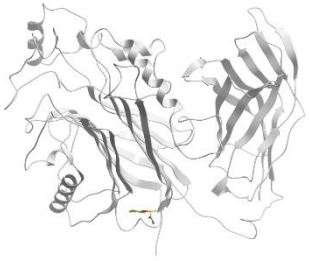	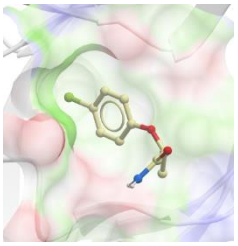	1.54
5RY3	x0469 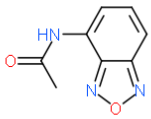	Site 01 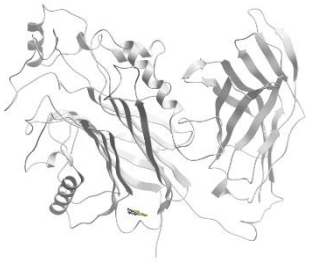	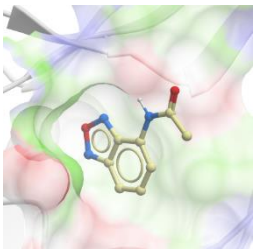	1.50
5RY4	x0479 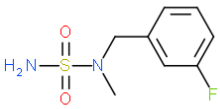	Site 01 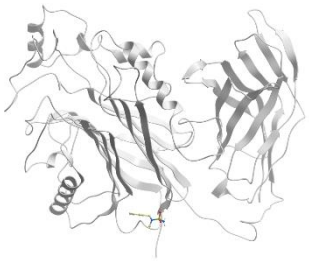	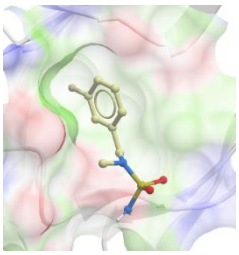	1.50
5RY6	x0494 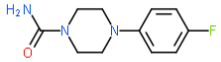	Site 01 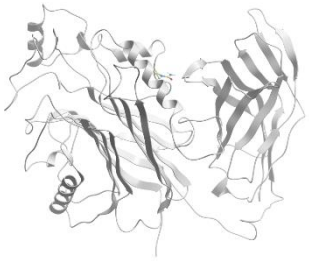	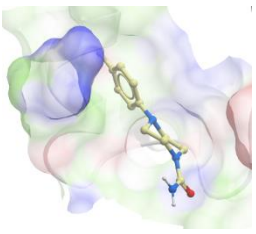	1.74
5RY8	x0518 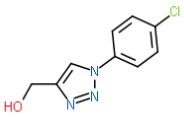	Site 01 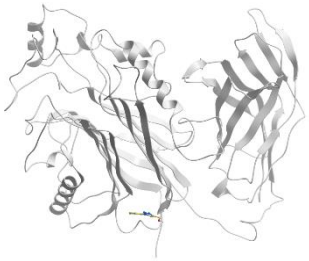	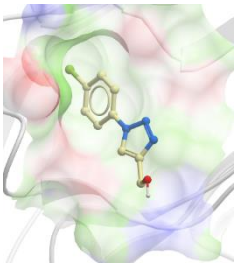	1.43

5RYD	x0558 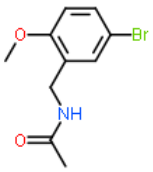	Site 01 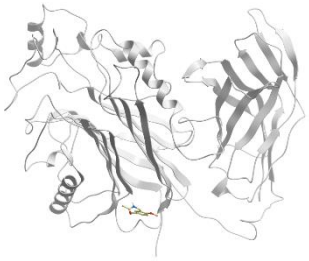	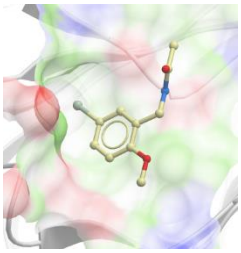	1.60
5RYE	x0560 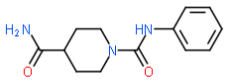	Site 01 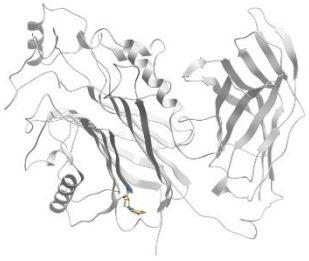	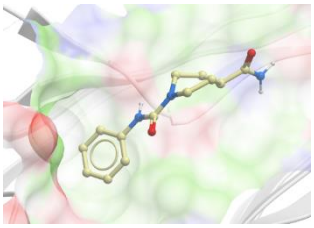	1.70
5RYL	x0609 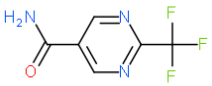	Site 01 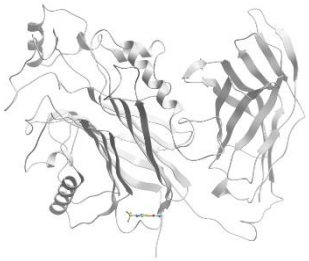	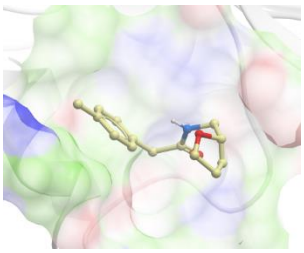	1.55
5RW3	x0020 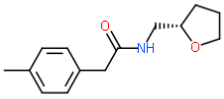	Site 02 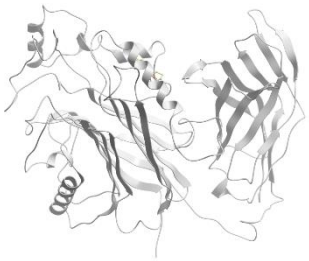	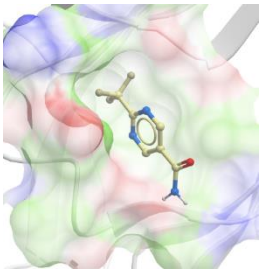	1.37
5RWA	x0058 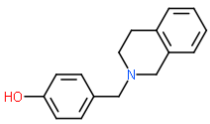	Site 02 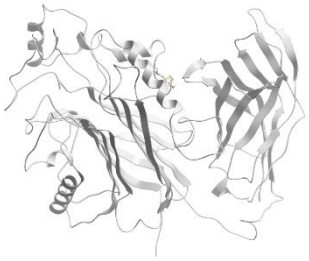	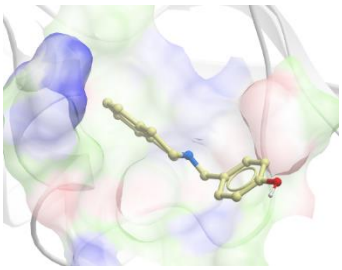	1.29
5RWC	x0067	Site 02 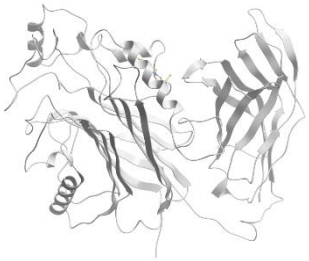	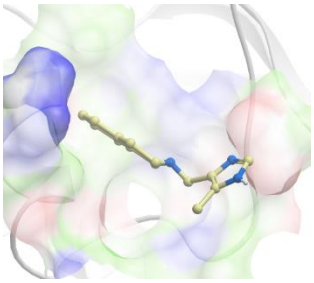	1.40

	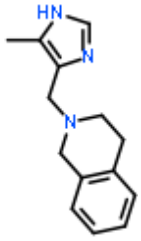			
5RWE	x0075 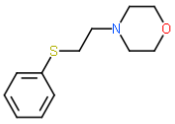	Site 02 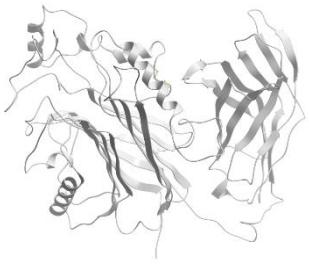	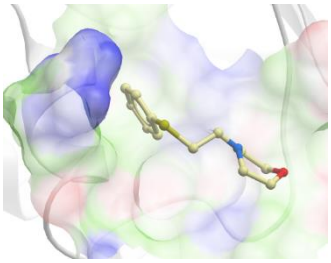	1.34
5RWF	x0083 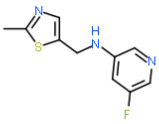	Site 02 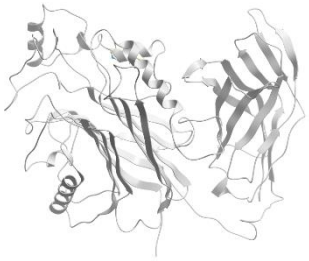	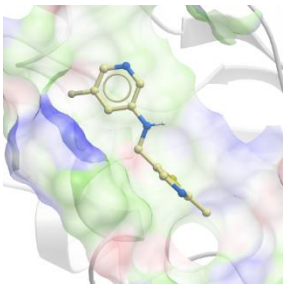	1.35
5RWH	x0088 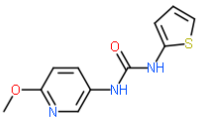	Site 02 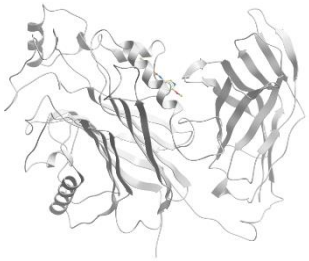	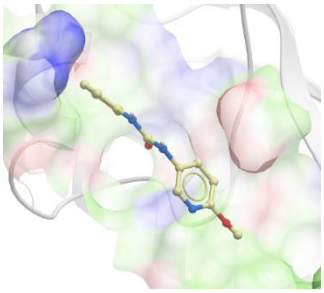	1.56
5RWI	x0092 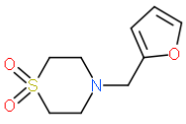	Site 02 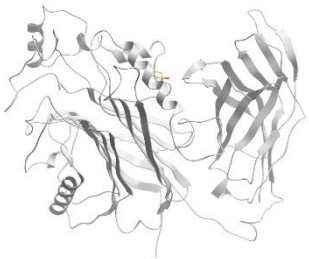	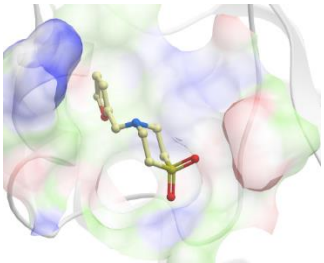	1.29
5RWO	x0114 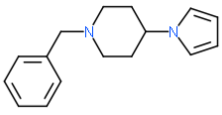	Site 02	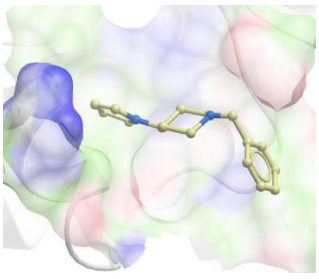	1.29

		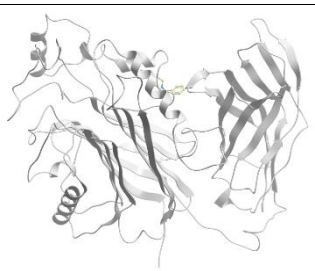		
5RWQ	x0119 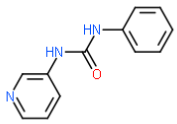	Site 02 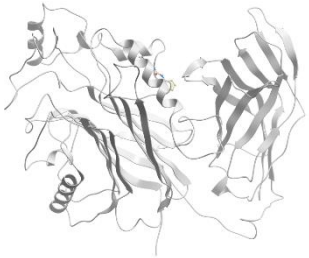	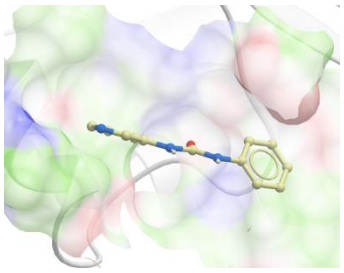	1.32
5RWS	x0126 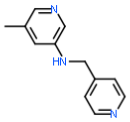	Site 02 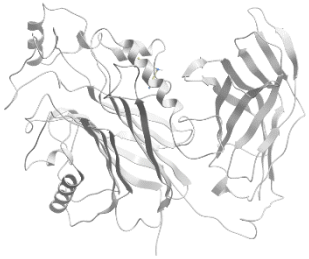	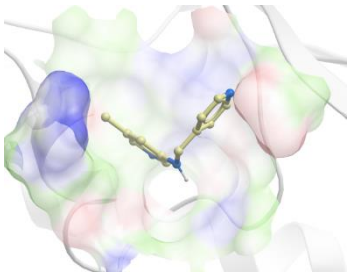	1.28
5RWT	x0129 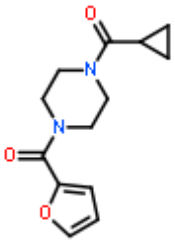	Site 02 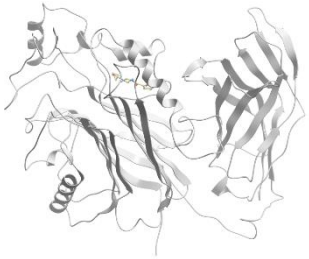	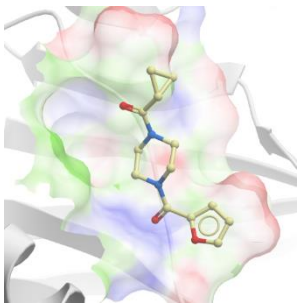	1.43
5RWV	x0140 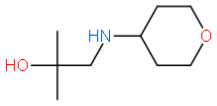	Site 02 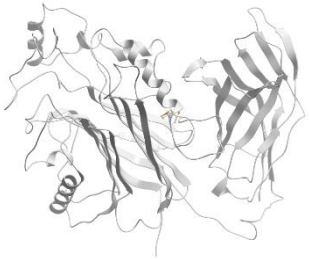	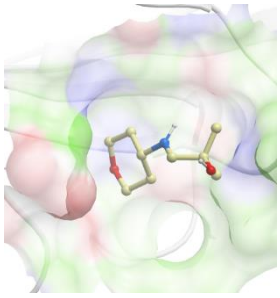	1.25
5RWW	x0141 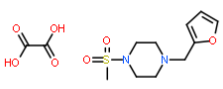	Site 02 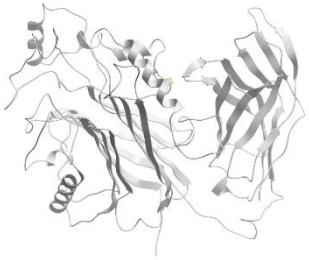	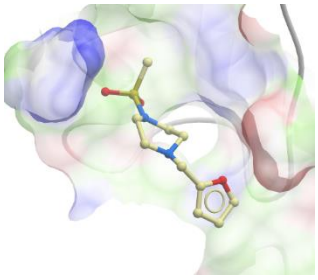	1.16

5RWY	x0152 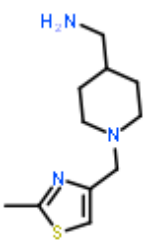	Site 02 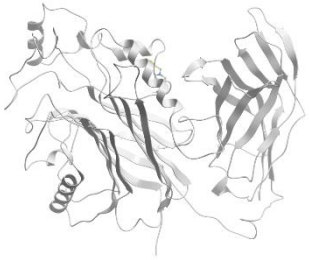	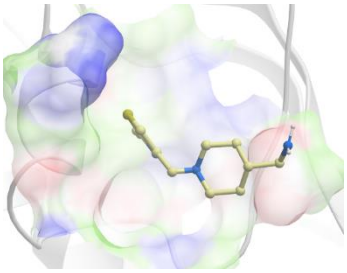	1.35
5RWZ	x0154 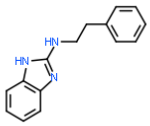	Site 02 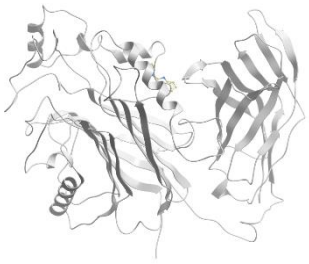	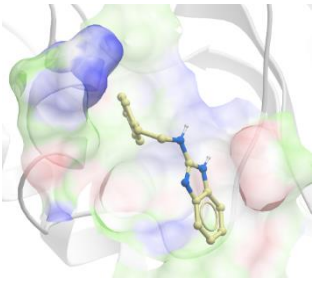	1.42
5RX1	x0163 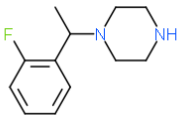	Site 02 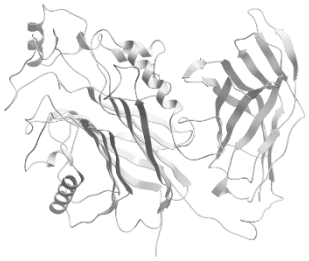	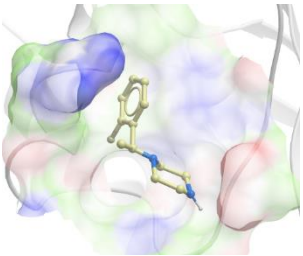	1.31
5RX3	x0174 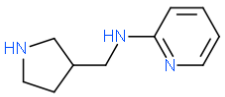	Site 02 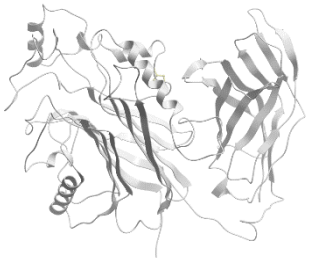	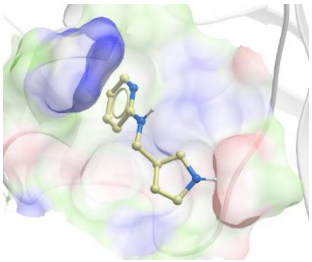	1.45
5RX4	x0176 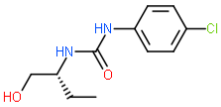	Site 02 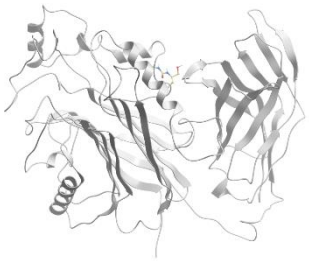	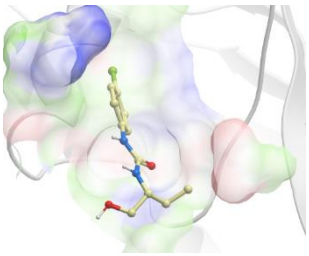	1.35
5RX7	x0194	Site 02	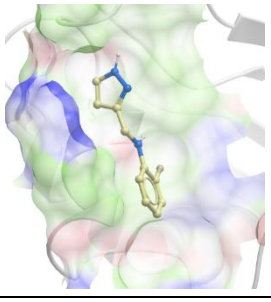	1.36

	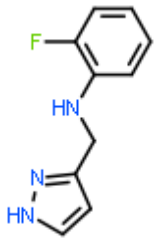	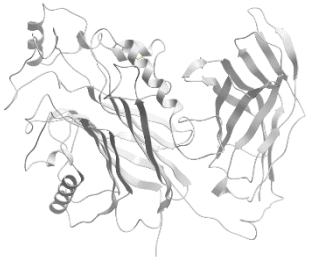		
5RX8	x0195 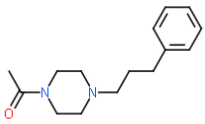	Site 02 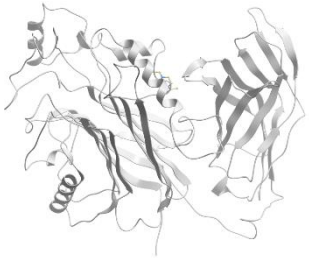	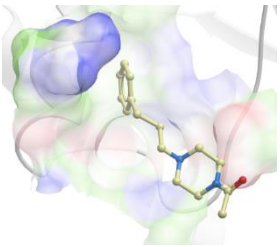	1.34
5RX9	x0200 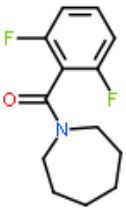	Site 02 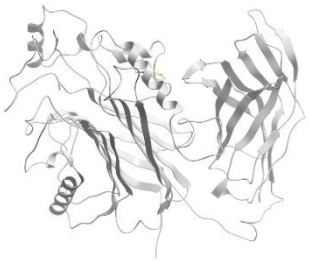	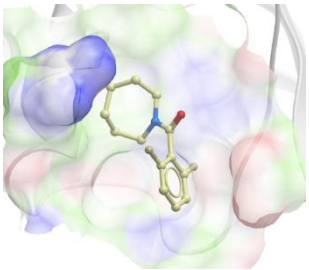	1.29
5RXA	x0201 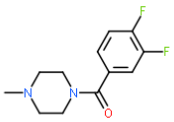	Site 02 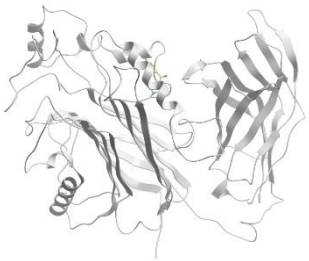	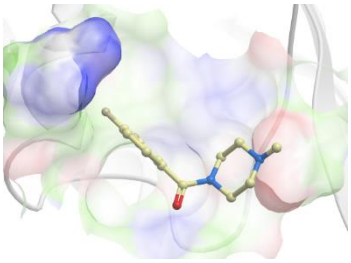	1.24
5RXB	x0221 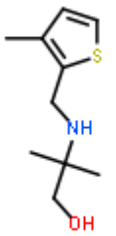	Site 02 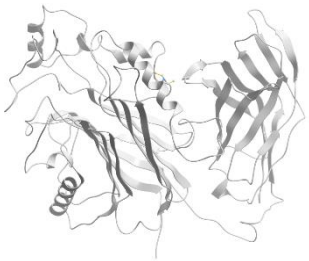	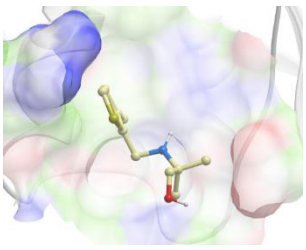	1.58
5RXC	x0239 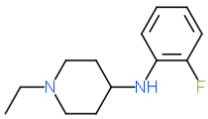	Site 02 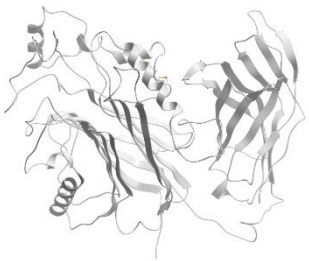	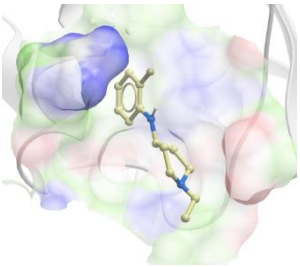	1.59

5RXG	x0302 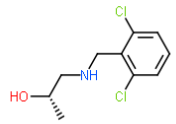	Site 02 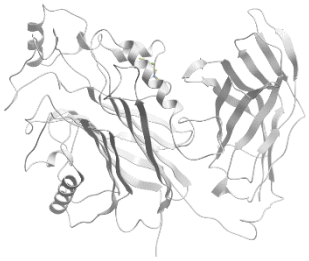	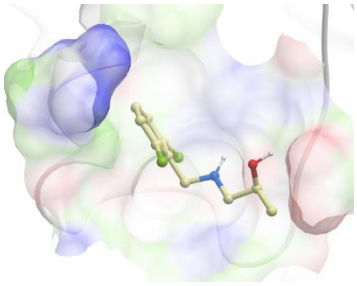	1.52
5RXH	x0303 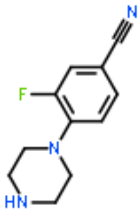	Site 02 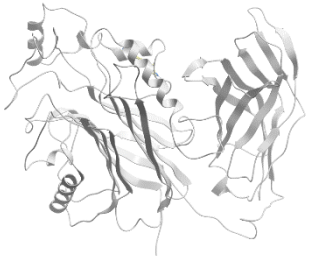	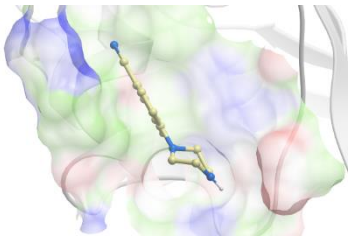	1.42
5RXI	x0311 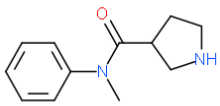	Site 02 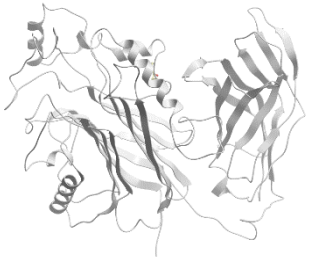	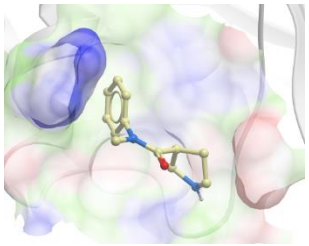	1.74
5RXJ	x0316 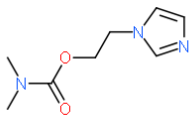	Site 02 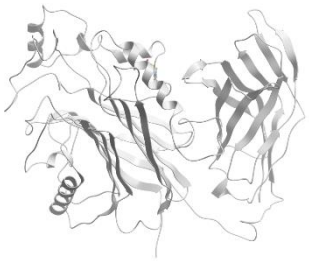	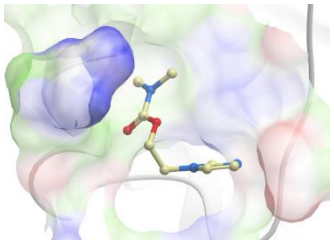	1.52
5RXK	x0320 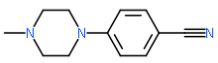	Site 02 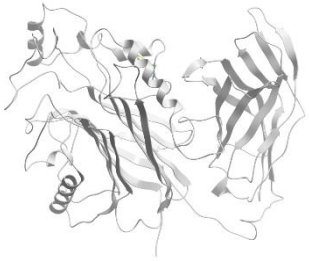	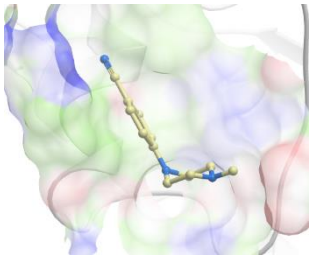	1.46
5RXM	x0340 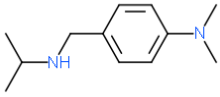	Site 02 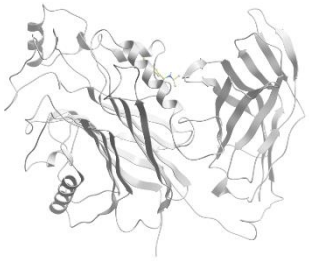	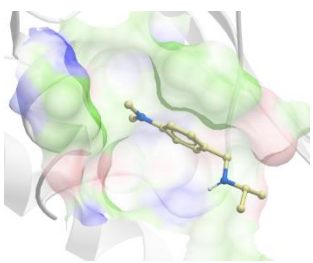	1.46

5RXR	x0358 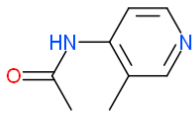	Site 02 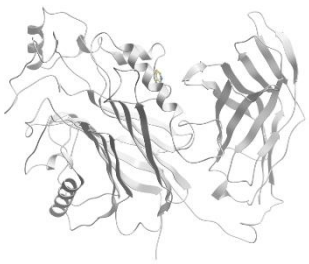	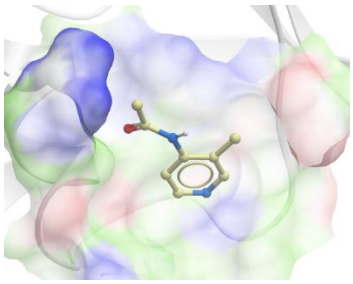	1.40
5RXU	x0368 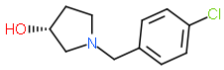	Site 02 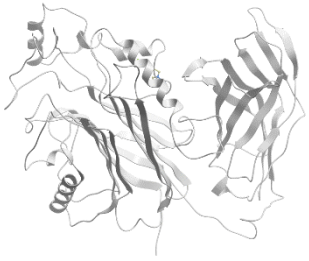	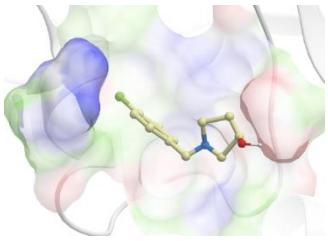	1.64
5RXX	x0401 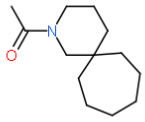	Site 02 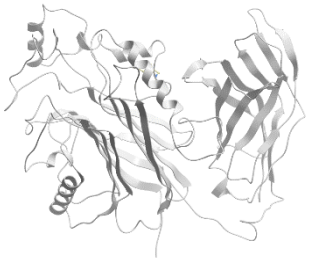	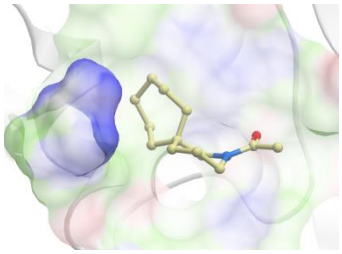	1.43
5RXY	x0403 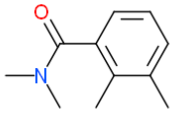	Site 02 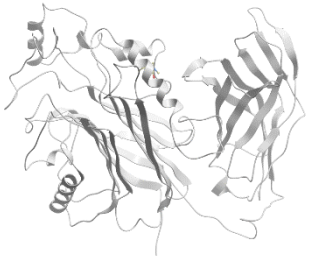	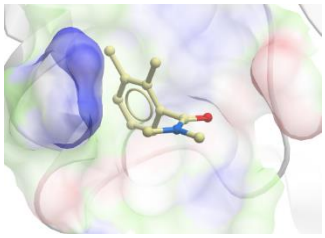	1.40
5RY5	x0490 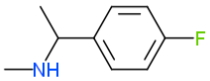	Site 02 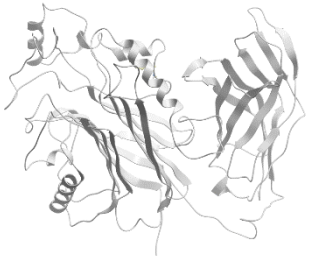	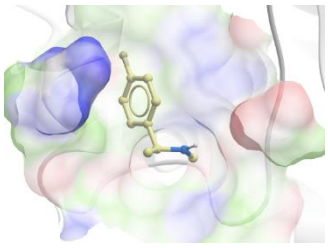	1.54
5RY7	x0510 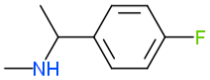	Site 02 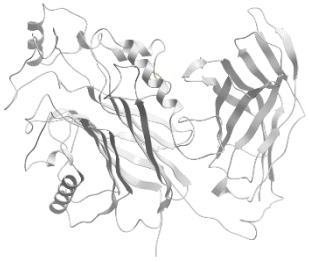	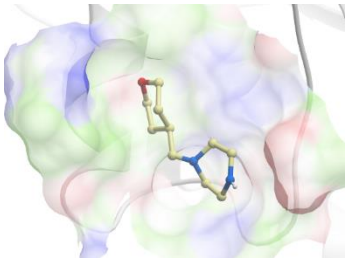	1.60

5RYA	x0527 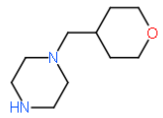	Site 02 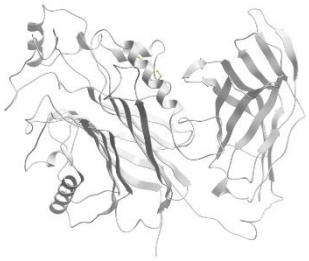	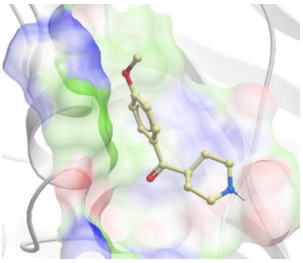	1.32
5RYF	x0573 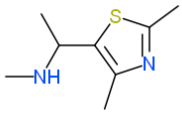	Site 02 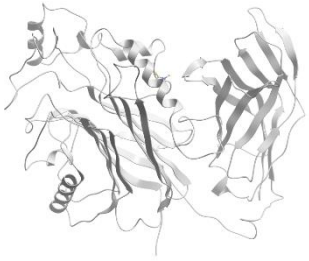	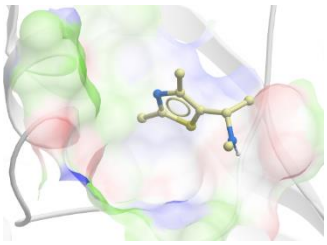	1.49
5RYH	x0588 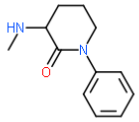	Site 02 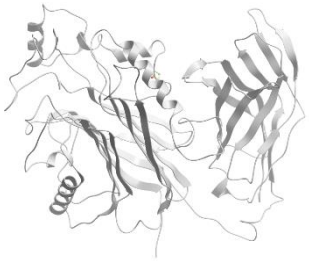	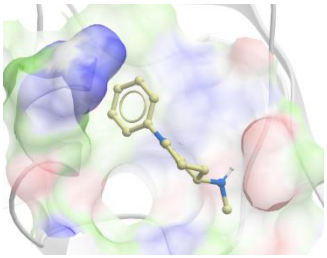	1.72
5RYI	x0590 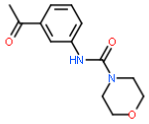	Site 02 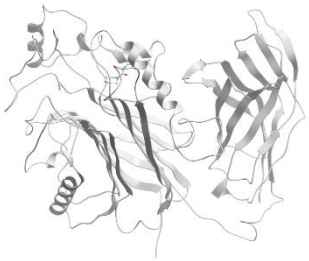	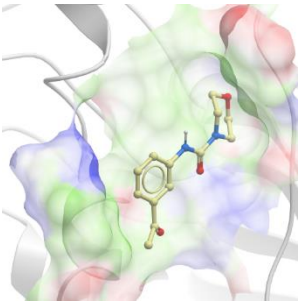	1.45
5RYK	x0604 	Site 02 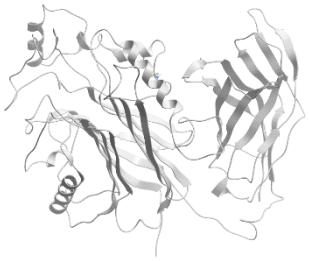	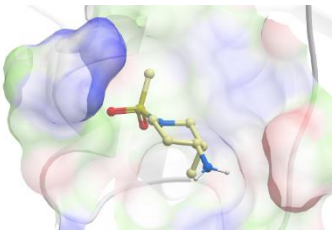	1.55
5RWD	x0073 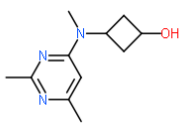	Site 03 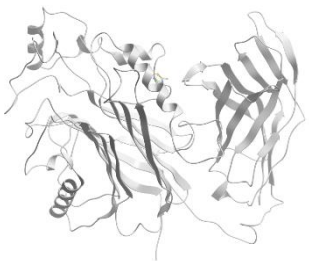	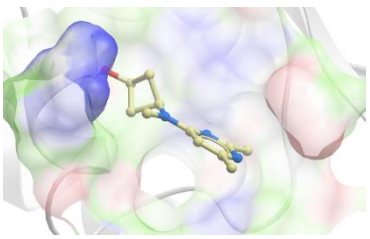	1.29

5RWL	x0101 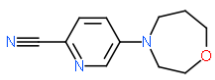	Site 03 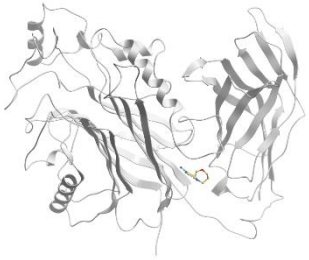	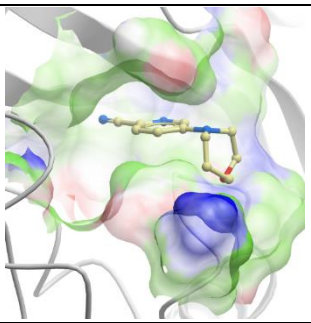	1.37
5RXV	x0378 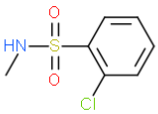	Site 03 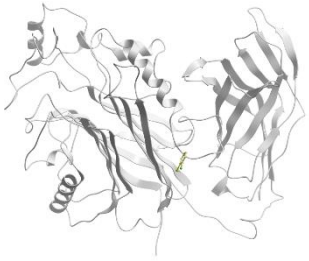	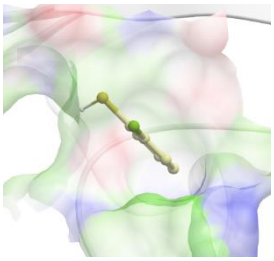	1.50
5RY9	x0524 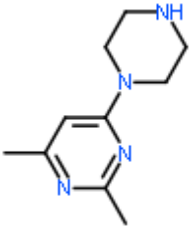	Site 03 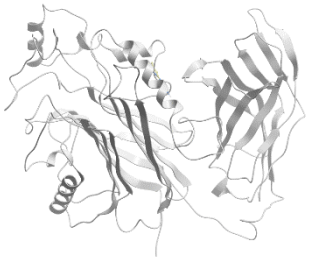	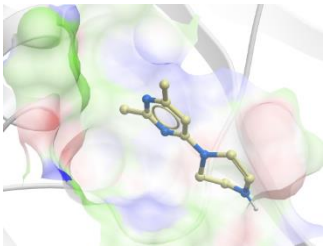	1.52
5RYC	x0543 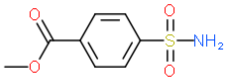	Site 03 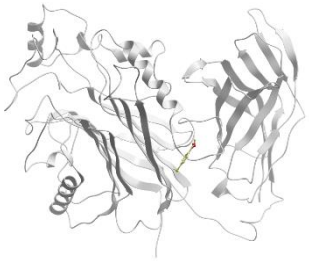	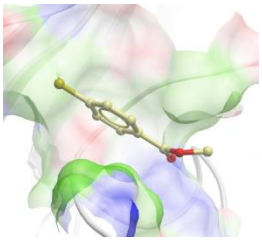	1.56
5RW5	x0027 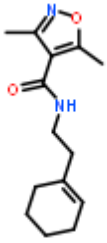	Site 04 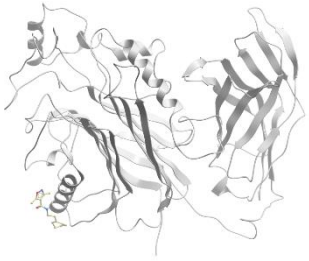	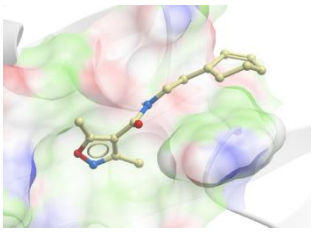	1.38

5RWN	x0106 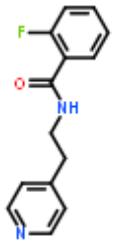	Site 04 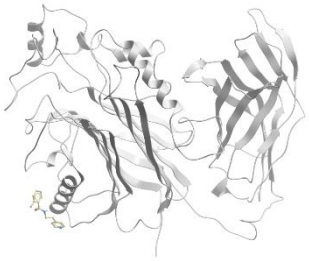	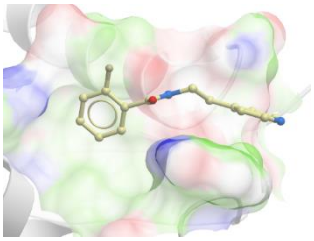	1.38
5RWU	x0133 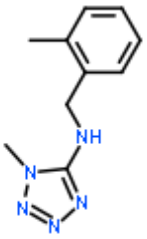	Site 04 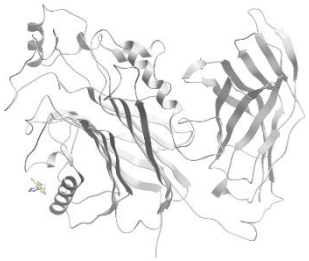	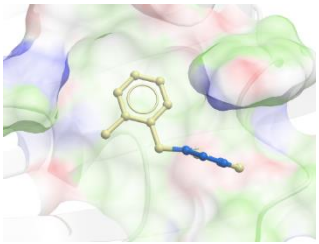	1.37
5RX0	x0161 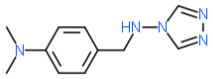	Site 04 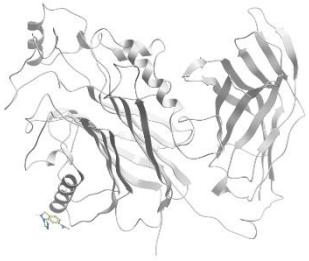	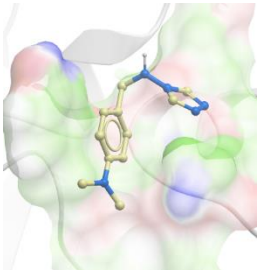	1.43
5RXL	x0325 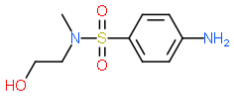	Site 04 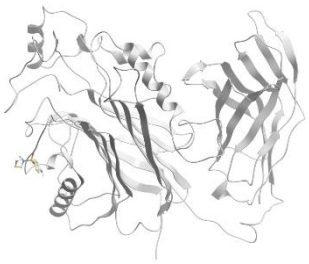	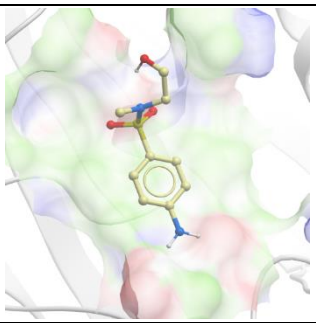	1.49
5RYG	x0577 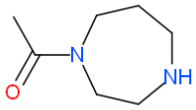	Site 04 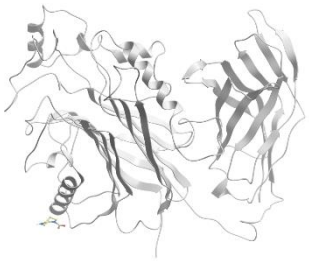	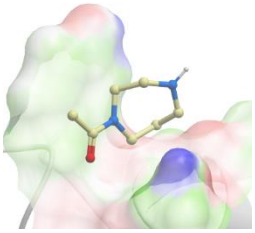	1.47

5RYJ	x0596 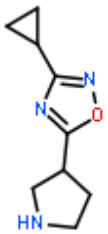	Site 04 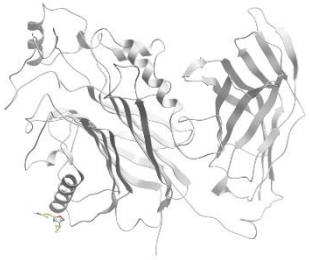	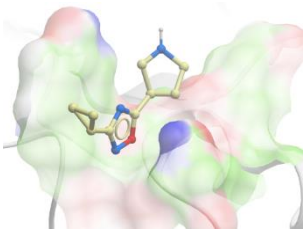	1.42
5RWB	x0062 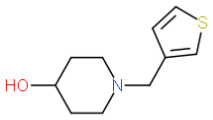	Site 05 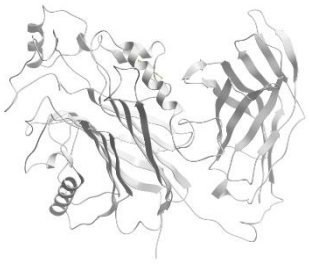	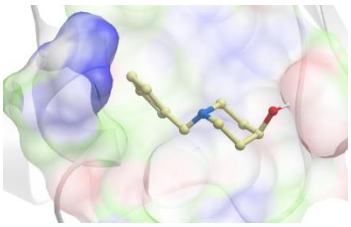	1.25
5RWM	x0103 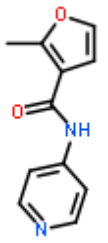	Site 07 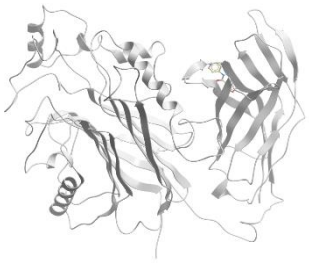	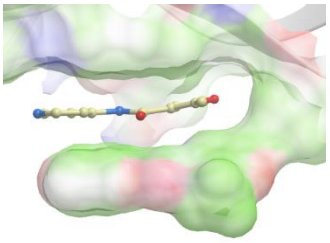	1.36
5RWX	x0148 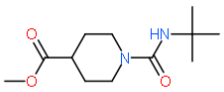	Site 08 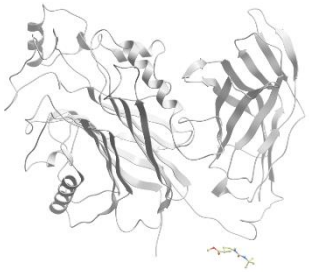	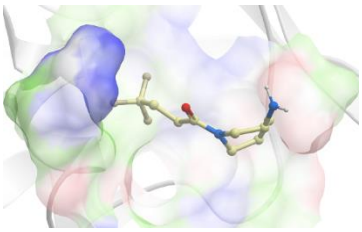	1.34
5RXS	x0359 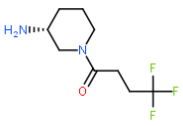	Site 08 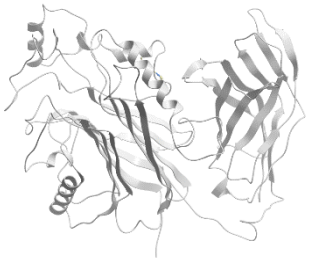	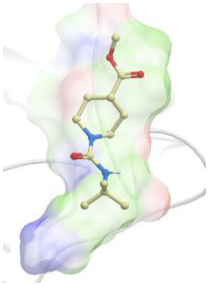	1.37

5RX5	x0182 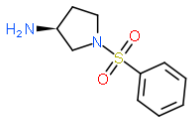	Site 09 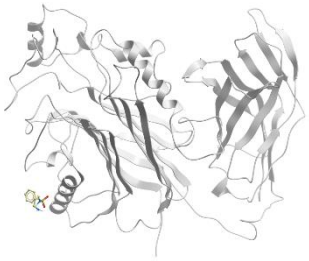	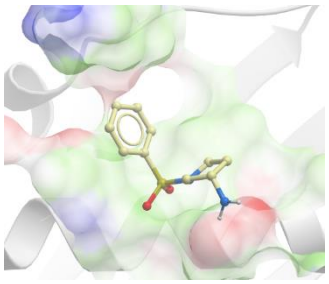	1.28
5RY1	x0438 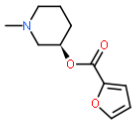	Site 10 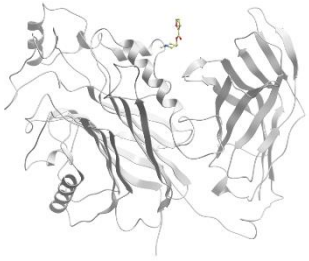	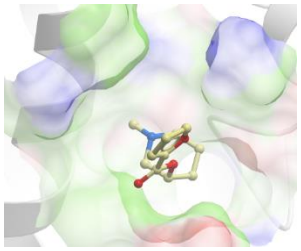	1.52
5RYB	x0542 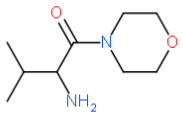	Site 12 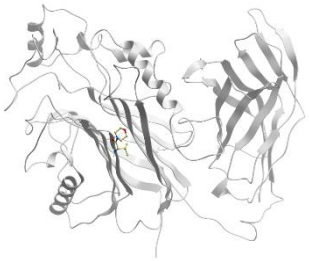	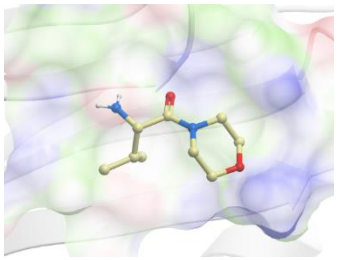	1.55

Materials and Methods

Cloning and expression

Expression plasmids

INPP5DA-c232 (Phosphatase and C2 domains 396-856). Vector: pFB-HGT-LIC (Baculovirus transfer vector with N-terminal His6-GST-TEV tag. Ampicillin -resistance). The plasmid is recombined with a baculovirus genome using the Bac-to-Bac system (Thermo), and the DNA is transfected into SF9 cells for virus generation and propagation.

Protein sequence with tag (Tag sequence underlined; * TEV protease cleavage site)

*MGHHHHHHSSMSPILGYWKIKGLVQPTRLLLEYLEEKYEEHLYERDEGDKWRNKKFELGLEFPNLPYYIDGDVKLTQSMAIIR YIADKHNMLGGCPKERAEISMLEGAVLDIRYGVSRIAYSKDFETLKVDFLSKLPEMLKMFEDRLCHKTYLNGDHVTHPDFMLY DALDVVLYMDPMCLDAFPKLVCFKKRIEAIPQIDKYLKSSKYIAWPLQGWQATFGGGDHPPKSSSGVDLGTENLYFQ*SM*E QPEPDMITIFIGTWNMGNAPPPKKITSWFLSKGQGKTRDDSADYIPHDIYVIGTQEDPLSEKEWLEILKHSLQEITSVTFKTVAI HTLWNIRIVVLAKPEHENRISHICTDNVKTGIANTLGNKGAVGVSFMFNGTSLGFVNSHLTSGSEKKLRRNQNYMNILRFLAL GDKKLSPFNITHRFTHLFWFGDLNYRVDLPTWEAETIIQKIKQQQYADLLSHDQLLTERREQKVFLHFEEEEITFAPTYRFERLT RDKYAYTKQKATGMKYNLPSWCDRVLWKSYPLVHVVCQSYGSTSDIMTSDHSPVFATFEAGVTSQFVSKNGPGTVDSQGQ IEFLRCYATLKTKSQTKFYLEFHSSCLESFVKSQEGENEEGSEGELVVKFGETLPKLKPIISDPEYLLDQHILISIKSSDSDESYGEGCI ALRLEATETQLPIYTPLTHHGELTGHFQGEIKLQTSQ

Predicted mass: 81077.6

Protein sequence after tag removal:

SMEQPEPDMITIFIGTWNMGNAPPPKKITSWFLSKGQGKTRDDSADYIPHDIYVIGTQEDPLSEKEWLEILKHSLQEITSVTFK
TVAIHTLWNIRIVVLAKPEHENRISHICTDNVKTGIANTLGNKGAVGVSFMFNGTSLGFVNSHLTSGSEKKLRRNQNYMNILR
FLALGDKKLSPFNITHRFTHLFWFGDLNYRVDLPTWEAETIIQKIKQQQYADLLSHDQLLTERREQKVFLHFEEEEITFAPTYRF
ERLTRDKYAYTKQKATGMKYNLPSWCDRVLWKSYPLVHVVCQSYGSTSDIMTSDHSPVFATFEAGVTSQFVSKNGPGTVDS
QGQIEFLRCYATLKTKSQTKFYLEFHSSCLESFVKSQEGENEEGSEGELVVKFGETLPKLKPIISDPEYLLDQHILISIKSSDSDESY
GEGCIALRLEATETQLPIYTPLTHHGELTGHFQGEIKLQTSQ

Predicted mass: 52812.9

DNA sequence (ORF):
ATGGGCCACCATCATCATCATCATTCTTCTATGTCCCCTATACTAGGTTATTGGAAAATTAAGGGCCTTGTGCAACCCACT
CGACTTCTTTTGGAATATCTTGAAGAAAAATATGAAGAGCATTTGTATGAGCGCGATGAAGGTGATAAATGGCGAAAC
AAAAAGTTTGAATTGGGTTTGGAGTTTCCCAATCTTCCTTATTATATTGATGGTGATGTTAAATTAACACAGTCTATGGC
CATCATACGTTATATAGCTGACAAGCACAACATGTTGGGTGGTTGTCCAAAAGAGCGTGCAGAGATTTCAATGCTTGAA
GGAGCGGTTTTGGATATTAGATACGGTGTTTCGAGAATTGCATATAGTAAAGACTTTGAAACTCTCAAAGTTGATTTTCT
TAGCAAGCTACCTGAAATGCTGAAAATGTTCGAAGATCGTTTATGTCATAAAACATATTTAAATGGTGATCATGTAACCC
ATCCTGACTTCATGTTGTATGACGCTCTTGATGTTGTTTTATACATGGACCCAATGTGCCTGGATGCGTTCCCAAAATTA
GTTTGTTTTAAAAAACGTATTGAAGCTATCCCACAAATTGATAAGTACTTGAAATCCAGCAAGTATATAGCATGGCCTTT
GCAGGGCTGGCAAGCCACGTTTGGTGGTGGCGACCATCCTCCAAAATCGAGCTCAGGTGTAGATCTGGGTACCGAGAA
CCTGTACTTCCAATCCATGGAGCAGCCGGAGCCCGACATGATCACCATCTTCATCGGCACCTGGAACATGGGTAACGCC
CCCCCTCCCAAGAAGATCACGTCCTGGTTTCTCTCCAAGGGGCAGGGAAAGACGCGGGACGACTCTGCGGACTACATC
CCCCATGACATTTACGTGATCGGCACCCAAGAGGACCCCCTGAGTGAGAAGGAGTGGCTGGAGATCCTCAAACACTCC
CTGCAAGAAATCACCAGTGTGACTTTTAAAACAGTCGCCATCCACACGCTCTGGAACATCCGCATCGTGGTGCTGGCCA
AGCCTGAGCACGAGAACCGGATCAGCCACATCTGTACTGACAACGTGAAGACAGGCATTGCAAACACACTGGGGAACA
AGGGAGCCGTGGGGGTGTCGTTCATGTTCAATGGAACCTCCTTAGGGTTCGTCAACAGCCACTTGACTTCAGGAAGTG
AAAAGAAACTCAGGCGAAACCAAAACTATATGAACATTCTCCGGTTCCTGGCCCTGGGCGACAAGAAGCTGAGTCCCTT
TAACATCACTCACCGCTTCACGCACCTCTTCTGGTTTGGGGATCTTAACTACCGTGTGGATCTGCCTACCTGGGAGGCAG
AAACCATCATCCAGAAAATCAAGCAGCAGCAGTACGCAGACCTCCTGTCCCACGACCAGCTGCTCACAGAGAGGAGGG
AGCAGAAGGTCTTCCTACACTTCGAGGAGGAAGAAATCACGTTTGCCCCAACCTACCGTTTTGAGAGACTGACTCGGGA
CAAATACGCCTACACCAAGCAGAAAGCGACAGGGATGAAGTACAACTTGCCTTCCTGGTGTGACCGAGTCCTCTGGAA
GTCTTATCCCCTGGTGCACGTGGTGTGTCAGTCTTATGGCAGTACCAGCGACATCATGACGAGTGACCACAGCCCTGTC
TTTGCCACATTTGAGGCAGGAGTCACTTCCCAGTTTGTCTCCAAGAACGGTCCCGGGACTGTTGACAGCCAAGGACAGA
TTGAGTTTCTCAGGTGCTATGCCACATTGAAGACCAAGTCCCAGACCAAATTCTACCTGGAGTTCCACTCGAGCTGCTTG
GAGAGTTTTGTCAAGAGTCAGGAAGGAGAAAATGAAGAAGGAAGTGAGGGGGAGCTGGTGGTGAAGTTTGGTGAGA
CTCTTCCAAAGCTGAAGCCCATTATCTCTGACCCTGAGTACCTGCTAGACCAGCACATCCTCATCAGCATCAAGTCCTCT
GACAGCGACGAATCCTATGGCGAGGGCTGCATTGCCCTTCGGTTAGAGGCCACAGAAACGCAGCTGCCCATCTACACG
CCTCTCACCCACCATGGGGAGTTGACAGGCCACTTCCAGGGGGAGATCAAGCTGCAGACCTCTCAGTGA

Note: in initial experiments, the same His6-GST-INPP5D(396-856) fusion protein was expressed in E. coli from construct INPP5DA-c132. This protein was used to generate the first crystal structure, 6IBD. This construct was supplanted by the baculovirus construct, which gives much higher yields and purity, in all subsequent experiments and structures (6XY7 and the fragment screen).

The protein was expressed in Sf9 cells grown in Sf-900 II SFM. Each litre of cells at a density of $0.2x10^6$/ml was infected with in 3 ml of P2 viruses and allowed to grow for approximately 68 hours at 27 °C. Cells were harvested by centrifugation at 1500g, flash frozen in liquid nitrogen and stored at -80 °C.

Protein purification

Purifications were performed on cell pellets from an expression volume of 1 or 2 litres. Pellets were resuspended in lysis buffer (50 mM HEPES pH 7.5, 500 mM NaCl, 20 mM imidazole, 5% glycerol, 1 mM TCEP) to a volume of 120 ml per litre expression. EDTA-free protease inhibitors were also added. The cells were lysed by sonication on ice with 5 seconds on, 10 seconds off for a total of 15 minutes. The lysate was mixed halfway through. Once lysis was complete, lysate was cleared by centrifugation at 75,000g for 20 minutes.

3 ml of nickel beads prewashed in lysis buffer were added to the supernatant, split between 50 ml falcon tubes, which were rotated in a cold room for 1 hour. The beads were pelleted by centrifugation at 700g for 5 minutes, resuspended in 50 ml lysis buffer, pelleted, then in resuspended in 50 ml and pelleted again.

The beads were resuspended in 20 ml lysis buffer and put on a gravity column. The column was washed with 10 ml wash buffer (50 mM HEPES pH 7.5, 500 mM NaCl, 40 mM imidazole, 5% glycerol, 1 mM TCEP) and the protein was eluted with three 10 ml washes with elution buffer (50 mM HEPES pH 7.5, 500 mM NaCl, 300 mM imidazole, 5% glycerol, 1 mM TCEP).

TEV protease was added to the eluate at a concentration (mg/ml) of 5:1 target protein:TEV (This concentration was required for INPP5DA-c232 and INPPL1A-c232, but not for other inositol phosphatases in the selectivity panel. The mixture was dialysed overnight into dialysis buffer (50 mM HEPES pH 7.5, 500 mM NaCl, 5% glycerol, 1 mM TCEP) at 4 °C.

The TEV was removed by passing the sample back down the nickel column, which was washed with 10 ml lysis buffer. The flow through and wash fractions were combined and concentrated to a volume of 1 ml. This was passed down a Superdex 200 16/60 column in gel filtration buffer (50 mM HEPES pH 7.5, 250 mM NaCl, 5% glycerol, 1 mM TCEP). Selected fractions were combined and concentrated.

Crystallisation

Crystallisation conditions were screened at 20 °C by sitting drop vapour diffusion using 150 nl drops with ratios of 2:1, 1:1 and 1:2. Screens were set up around identified conditions. Apo SHIP1 crystals grew from protein at 6 mg/ml in 0.1M bis-tris pH 7.0, 14% PEG2KMME, 12% PEG3350. The crystals were cryoprotected by addition of 1 µl reservoir to the drop. These crystals were also used for seeding. Crystals from 6 drops were resuspended in a total of 30 µl reservoir solution and conditions were rescreened with 20 nl seeds added to 150 nl drops. Crystals were observed in Molecular Dimensions Morpheus C1 (30 mM sodium phosphate, ammonium sulphate, sodium nitrate, 100 mM MES/imidazole pH 6.5, 10% PEG 20,000, 20 % PEG 500 MME) after around a week. Crystals grown in this way were used for X-ray fragment screens at Diamond Light Source using the standard X-Chem protocol with fragment soaks at 75 mM (15% DMSO) (19). Crystals were harvested after approximately 2.5 to 5 hours. Alternatively, they were cryoprotected by addition of 1 µl reservoir solution to the drop with 2mM $MgCl_2$ added to obtain the magnesium and phosphate bound structure. SHIP2 crystals were obtained in the same form as the published SHIP2 structure (5OKM) (10) in 2.4 M sodium malonate, pH 7.0 mixed 9:1 with a wide range of PEG containing conditions. The crystals were cryoprotected by addition of 1 µl reservoir solution.

Data collection and processing

Data collection: For the apo structure 6IBD, data were collected at Diamond Light Source on beamline I03 to a resolution of 1.48 Å. For the magnesium and phosphate bound structure 6XY7, data were also collected on I03 to a resolution of 1.09 Å.

Data processing: The data were integrated with Dials and scaled with Aimless. For the magnesium and phosphate bound structure 6XY7, an anisotropic high-resolution limit of 1.09-1.34 Å was applied using Staraniso. Both structures were determined by molecular replacement with Phaser using the phosphatase domains of SHIP2 (5OKM, chain B) as a model. The structures were refined using Refmac to final R / R_{free} of 17.3%/20.0% and 13.6%/15.9% for 6IBD and 6XY7, respectively.

Malachite green assay

The assay was performed in a 384-well clear-bottomed, black-walled microtitre plate (Greiner Bio One, # - 781906). Additions of INPP5D enzyme dilution, test compound and INPP5D substrate phosphatidylinositol (3,4,5)-trisphosphate (Echelon Biosciences, # - P-3908) were made to a final assay volume of 40 µL/well. The [final] for substrate was 50 µM. The known INPP5D catalytic activity inhibitors 3AC (Calbiochem, # - 565835)

or K118 (Echelon Biosciences, # - B-0344) were used as positive controls for inhibition at a [final] of ≥ 100 µM. After 30 min incubation at room temperature, the assay was terminated and detection performed using the Malachite Green Phosphate Assay Kit (Sigma-Aldrich, # - MAK307). Detection solution was prepared to the required volume by combining 100 volumes of Reagent A to 1 volume of Reagent B. Detection solution was added to test wells 10 µL/well, followed by 30 min incubation at room temperature. The signal was determined by measuring Abs^{620nm} using the PHERAstar FS (BMG Labtech).

References

1. Brauer, H., Strauss, J., Wegner, W., Muller-Tidow, C., Horstmann, M., and Jucker, M. (2012) Leukemia-associated mutations in SHIP1 inhibit its enzymatic activity, interaction with the GM-CSF receptor and Grb2, and its ability to inactivate PI3K/AKT signaling. *Cell Signal* **24**, 2095-2101
2. Kandell, W. M., Donatelli, S. S., Trinh, T. L., Calescibetta, A. R., So, T., Tu, N., Gilvary, D. L., Chen, X., Cheng, P., Adams, W. A., Chen, Y. K., Liu, J., Djeu, J. Y., Wei, S., and Eksioglu, E. A. (2020) MicroRNA-155 governs SHIP-1 expression and localization in NK cells and regulates subsequent infiltration into murine AT3 mammary carcinoma. *PLoS One* **15**, e0225820
3. Miller, T. W., Rexer, B. N., Garrett, J. T., and Arteaga, C. L. (2011) Mutations in the phosphatidylinositol 3-kinase pathway: role in tumor progression and therapeutic implications in breast cancer. *Breast Cancer Res* **13**, 224
4. Ishihara, H., Sasaoka, T., Hori, H., Wada, T., Hirai, H., Haruta, T., Langlois, W. J., and Kobayashi, M. (1999) Molecular cloning of rat SH2-containing inositol phosphatase 2 (SHIP2) and its role in the regulation of insulin signaling. *Biochem Biophys Res Commun* **260**, 265-272
5. Marcano, A. C., Burke, B., Gungadoo, J., Wallace, C., Kaisaki, P. J., Woon, P. Y., Farrall, M., Clayton, D., Brown, M., Dominiczak, A., Connell, J. M., Webster, J., Lathrop, M., Caulfield, M., Samani, N., Gauguier, D., and Munroe, P. B. (2007) Genetic association analysis of inositol polyphosphate phosphatase-like 1 (INPPL1, SHIP2) variants with essential hypertension. *J Med Genet* **44**, 603-605
6. Paraiso, K. H., Ghansah, T., Costello, A., Engelman, R. W., and Kerr, W. G. (2007) Induced SHIP deficiency expands myeloid regulatory cells and abrogates graft-versus-host disease. *J Immunol* **178**, 2893-2900
7. Rosenthal, S. L., and Kamboh, M. I. (2014) Late-Onset Alzheimer's Disease Genes and the Potentially Implicated Pathways. *Curr Genet Med Rep* **2**, 85-101
8. Wilkins, H. M., Carl, S. M., Greenlief, A. C., Festoff, B. W., and Swerdlow, R. H. (2014) Bioenergetic dysfunction and inflammation in Alzheimer's disease: a possible connection. *Front Aging Neurosci* **6**, 311
9. Trésaugues, L., Silvander, C., Flodin, S., Welin, M., Nyman, T., Gräslund, S., Hammarström, M., Berglund, H., and Nordlund, P. (2014) Structural basis for phosphoinositide substrate recognition, catalysis, and membrane interactions in human inositol polyphosphate 5-phosphatases. *Structure* **22**, 744-755
10. Le Coq, J., Camacho-Artacho, M., Velazquez, J. V., Santiveri, C. M., Gallego, L. H., Campos-Olivas, R., Dolker, N., and Lietha, D. (2017) Structural basis for interdomain communication in SHIP2 providing high phosphatase activity. *Elife* **6**
11. Liu, Q., Shalaby, F., Jones, J., Bouchard, D., and Dumont, D. J. (1998) The SH2-containing inositol polyphosphate 5-phosphatase, ship, is expressed during hematopoiesis and spermatogenesis. *Blood* **91**, 2753-2759
12. Pesesse, X., Deleu, S., De Smedt, F., Drayer, L., and Erneux, C. (1997) Identification of a second SH2-domain-containing protein closely related to the phosphatidylinositol polyphosphate 5-phosphatase SHIP. *Biochem Biophys Res Commun* **239**, 697-700
13. Pedicone, C., Fernandes, S., Dungan, O. M., Dormann, S. M., Viernes, D. R., Adhikari, A. A., Choi, L. B., De Jong, E. P., Chisholm, J. D., and Kerr, W. G. (2020) Pan-SHIP1/2 inhibitors promote microglia effector functions essential for CNS homeostasis. *J Cell Sci* **133**
14. Jing, H., Zhu, J. X., Wang, H. F., Zhang, W., Zheng, Z. J., Kong, L. L., Tan, C. C., Wang, Z. X., Tan, L., and Tan, L. (2016) INPP5D rs35349669 polymorphism with late-onset Alzheimer's disease: A replication study and meta-analysis. *Oncotarget* **7**, 69225-69230

15. Stenton, G. R., Mackenzie, L. F., Tam, P., Cross, J. L., Harwig, C., Raymond, J., Toews, J., Wu, J., Ogden, N., MacRury, T., and Szabo, C. (2013) Characterization of AQX-1125, a small-molecule SHIP1 activator: Part 1. Effects on inflammatory cell activation and chemotaxis in vitro and pharmacokinetic characterization in vivo. *Br J Pharmacol* **168**, 1506-1518
16. Suwa, A., Yamamoto, T., Sawada, A., Minoura, K., Hosogai, N., Tahara, A., Kurama, T., Shimokawa, T., and Aramori, I. (2009) Discovery and functional characterization of a novel small molecule inhibitor of the intracellular phosphatase, SHIP2. *Br J Pharmacol* **158**, 879-887
17. Ong, C. J., Ming-Lum, A., Nodwell, M., Ghanipour, A., Yang, L., Williams, D. E., Kim, J., Demirjian, L., Qasimi, P., Ruschmann, J., Cao, L. P., Ma, K., Chung, S. W., Duronio, V., Andersen, R. J., Krystal, G., and Mui, A. L. (2007) Small-molecule agonists of SHIP1 inhibit the phosphoinositide 3-kinase pathway in hematopoietic cells. *Blood* **110**, 1942-1949
18. Savitsky, P., Bray, J., Cooper, C. D., Marsden, B. D., Mahajan, P., Burgess-Brown, N. A., and Gileadi, O. (2010) High-throughput production of human proteins for crystallization: the SGC experience. *J Struct Biol* **172**, 3-13
19. Pearce, N. M., Krojer, T., Bradley, A. R., Collins, P., Nowak, R. P., Talon, R., Marsden, B. D., Kelm, S., Shi, J., Deane, C. M., and von Delft, F. (2017) A multi-crystal method for extracting obscured crystallographic states from conventionally uninterpretable electron density. *Nat Commun* **8**, 15123

We respectfully request that this document is cited using the DOI value as given above if the content is used in your work.